4. Magnetic Reconnection

I am now going to switch gears and use the fact that I derived an expression for collisional resistivity of a plasma (as a pretext) to work through some key elements of the theory of magnetic reconnection — in its simplest (or at any rate best known and chronologically earlier, in parts) form, which is <u>resistive</u> reconnection. Resistivity in this context is the one effect that upsets MHD's ideal constraint on topological rearrangement of field lines (flux freezing). It turns out that quite a lot happens when these constraints can be broken, even when η is asymptotically small ($\to 0$).

To remind you about the part of MHD that will matter to us, Faraday's law tells us how magnetic field evolves:

$$\frac{\partial \vec{B}}{\partial t} = -c\nabla\times\vec{E} \tag{145}$$

and then, the MHD Ohm's law in the moving fluid element's frame is

$$\vec{E} + \frac{\vec{u}\times\vec{B}}{c} = \eta\vec{J} \tag{146}$$

Finally, Ampère's law neglecting displacement current (which is fine non-relativistically) is

$$\frac{4\pi}{c}\vec{j} = \nabla\times\vec{B} \tag{147}$$

Combining these equations, we get

$$\frac{\partial\vec{B}}{\partial t} = \nabla\times\left[\vec{u}\times\vec{B} - \frac{c^2\eta}{4\pi}\nabla\times\vec{B}\right] \tag{148}$$

We shall assume that we have derived η:

$$\eta = (\text{a number})\,\frac{m_e\nu_{ei}}{e^2 n_e} \quad \text{from §3.5}$$

$$= (\dots)\,\frac{Ze^2\Lambda_{ei}\,m_e^{1/2}}{T^{3/2}} \tag{149}$$

I say "assume" because in fact I only did it for a uniform static plasma, in the absence of $\vec{B}$. So actually more work is needed to put η into (148) legitimately – but I will do this work later, when I talk about Braginskii MHD (unless I run out of time).

I am now going to rename $\frac{c^2\eta}{4\pi} = \eta$ (we can't waste Greek letters, it's such a short alphabet!) and proceed.

$$\eta \sim \frac{Ze^2c^2\Lambda_{ei}\,m_e^{1/2}}{T^{3/2}} \sim \frac{\Lambda_{ei}}{N_D}\,d_e c \tag{150}$$

btw, [this is not, as far as I can tell, consequential].

If, furthermore, we can ignore the variations of T compared to the variations of B and so neglect $\nabla\eta$ terms, then (148) becomes

$$\frac{\partial \vec{B}}{\partial t} = \nabla\times(\vec{u}\times\vec{B}) + \eta\nabla^2\vec{B}, \qquad (151)$$

the familiar induction equation. The velocity field in it satisfies

$$\rho\left(\frac{\partial\vec{u}}{\partial t} + \vec{u}\cdot\nabla\vec{u}\right) = -\nabla p + \nabla\cdot\hat{\Pi} + \frac{(\nabla\times\vec{B})\times\vec{B}}{4\pi} \qquad (152)$$

viscous stress, which we will also ignore

In what follows, I will do further simplifications: everything in 2D and Ma ≪ 1 (subsonic, so approximately incompressible motions).

Then all dynamics can be described in terms of stream and flux functions:

$$\vec{u} = \hat{z}\times\nabla\Phi, \quad \vec{B} = \hat{z}\times\nabla\Psi, \qquad (153)$$

which satisfy

$$\begin{cases} \dfrac{\partial}{\partial t}\nabla_\perp^2\Phi + \{\Phi, \nabla_\perp^2\Phi\} = \{\Psi, \nabla_\perp^2\Psi\} & (154) \\[2ex] \dfrac{\partial\Psi}{\partial t} + \{\Phi, \Psi\} = \eta\nabla_\perp^2\Psi & (155) \end{cases}$$

These are 2D RMHD equations, which describe both what happens in literally 2D world and also in a plane $\perp$ strong mean field $\vec{B}_0 = B_0\hat{z}$ (in which case $\vec{B} = \vec{B}_0 + \delta\vec{B}$ and $\delta\vec{B} = \hat{z}\times\nabla\psi$), ignoring $\parallel$ propagation of Alfvén waves.

However restricted, this is a useful starting point – and one must start somewhere.

4.1 X-point Collapse

Let us consider a very simple solution of these equations, describing an "X-point":

$$\Phi_0(x,y) = \Gamma(t)\, x y \qquad (156)$$

$$\psi_0(x,y) = \frac{v_A}{2}\left[\frac{x^2}{a(t)} - \frac{y^2}{L(t)}\right] \qquad (157)$$

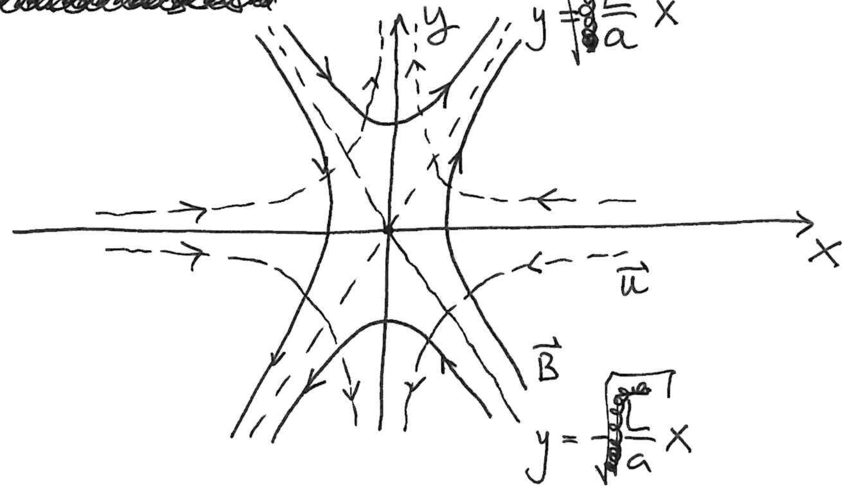

(154) is satisfied trivially (all terms = 0)

(155) becomes

$$-\left[\frac{x^2}{a^2}\frac{da}{dt} - \frac{y^2}{L^2}\frac{dL}{dt}\right] + \Gamma y\left(-\frac{2y}{L}\right) - \Gamma x\,\frac{2x}{a} =$$

$$= 2\eta\left(\frac{1}{a} - \frac{1}{L}\right) \to 0 \text{ if } \eta \to +0$$

$$\frac{1}{a}\frac{da}{dt} = -2\Gamma \quad\Rightarrow\quad a = a_0\, e^{-2\int_0^t dt'\,\Gamma(t')}$$

$$\frac{1}{L}\frac{dL}{dt} = 2\Gamma \quad\Rightarrow\quad L = L_0\, e^{2\int_0^t dt'\,\Gamma(t')} \qquad (158)$$

This was first proposed by Chapman & Kendall (1963), who, quite naturally, then considered $\Gamma = \Gamma_0 = \text{const}$.
This is actually not all that physical.
What the solution (158) describes is a tendency for an X-point in ideal MHD to "collapse", with "transverse" scale $a(t) \to 0$ and "longitudinal" scale $L(t) \to \infty$.

see Q5 of the MHD problem sheet

→ In compressible MHD, this is actually an explosive process, with the system collapsing to a line singularity along the y axis, known as the "current sheet" — "current" because along that singularity, $\vec{B}$ reverses over a small scale ($\to 0$) and the singularity will obviously be resolved in some way by resistivity:

$\frac{\eta}{a} \not\to 0$ as soon as

$$\frac{\eta}{a} \sim \frac{x^2}{a}\Gamma \Rightarrow x \sim \left(\frac{\eta}{\Gamma}\right)^{1/2} \qquad (159)$$

$$\text{So } a \sim \left(\frac{\eta}{\Gamma}\right)^{1/2}$$

Let us imagine that the outflow velocity at the end of the sheet is some constant parameter:

$$u_y = \frac{\partial \Phi_0}{\partial x} = \Gamma y = u_{out} \text{ at } y = L$$

$$\boxed{\Gamma(t) = \frac{u_{out}}{L(t)}} \qquad (160)$$

(fixed by some outside boundary conditions)

If it is not yet obvious to you that this is the right thing to assume, it will become obvious before this chapter is finished.

So then

$$\frac{1}{L}\frac{dL}{dt} = \frac{2u_{out}}{L} \Rightarrow \boxed{L = L_0 + 2u_{out}t} \qquad (161)$$

and

$$a = a_0 e^{-2\int_0^t dt' \frac{u_{out}}{L_0 + 2u_{out}t'}} = \frac{a_0 L_0}{L_0 + 2u_{out}t}, \qquad (162)$$

the Uzdensky–Loureiro (2016) solution.

With this solution in hand, we can recast the estimate (159) as follows:

$$\frac{L}{a} \sim L\left(\frac{\Gamma}{\eta}\right)^{1/2} \sim L\left(\frac{u_{out}}{L\eta}\right)^{1/2} \sim \left(\frac{L u_{out}}{\eta}\right)^{1/2} \equiv S_L^{1/2} \gg 1 \qquad (162a)$$

if $u_{out} = V_A$ (it is!), this is called Lundquist #

So evolution will cease to be ideal as soon as the aspect ratio of the sheet reaches $\sim S_L^{1/2}$, which it inevitably will because

$$\underbrace{\frac{L}{a} \propto L^2}_{(162)} \quad \text{and} \quad S_L^{1/2} \propto L^{1/2}$$

$$\frac{L^2}{a_0 L_0} \sim \frac{(L u_{out})^{1/2}}{\eta^{1/2}} \Rightarrow L = a_0^{2/3} L_0^{1/3} S_{L_0}^{1/3}$$

Let us now study a resistive sheet that has reached (162a).

4.2 Sweet-Parker Sheet

We now imagine a collapsed sheet, embedded in some global configuration, where the Chapman-Kendall-Uzdensky-Loureiro solution has reached some L and a for which (162a) is satisfied:

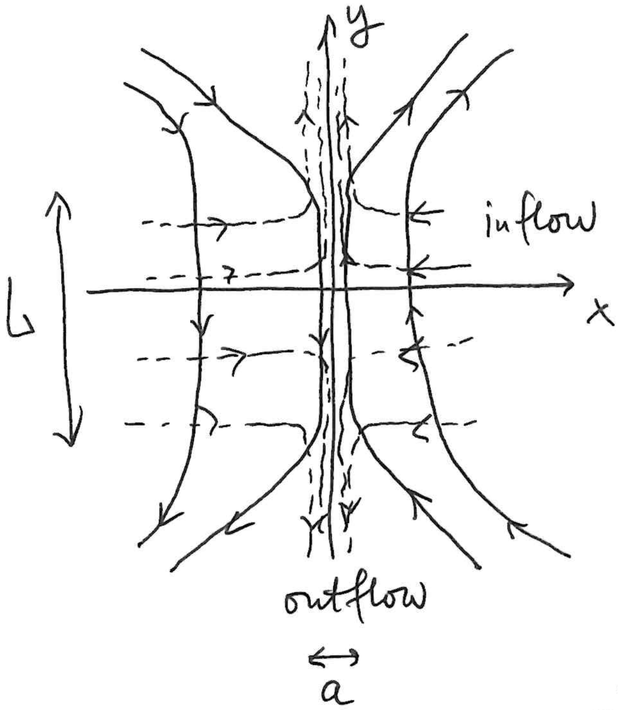

We do not need to be tethered to the solution (156–157) to see what everything is here.

Inside the sheet, we have

$$\{\Phi, \psi\} \sim \eta \nabla_\perp^2 \psi \qquad \partial_y^2 \ll \partial_x^2$$

$$\partial_x \Phi\, \partial_y \psi - \partial_y \Phi\, \partial_x \psi \qquad\qquad \eta\, \partial_x^2 \psi$$

$$= -\cancel{u_y B_x} + u_x B_y \qquad\qquad \eta\, \partial_x B_y$$

$$0 \qquad\qquad u_{in} V_A \qquad\qquad \eta \frac{V_A}{\delta}$$

0: not much of that coming into sheet

V_A: upstream (incoming) field

δ: width of sheet (formerly a, now denoted δ because small)

$$\delta \sim \frac{\eta}{u_{in}} \qquad (162b)$$

But mass is conserved and flow is incompressible, so

$$u_{in} L \sim u_{out} \delta \qquad (162c)$$

whence

$$\delta \sim \frac{\eta L}{u_{out} \delta} \Rightarrow \boxed{\delta \sim \left(\frac{\eta L}{u_{out}}\right)^{1/2} \sim L\, S_L^{-1/2}} \qquad (162d)$$

the result we already had in (162a)

[this is just a rederivation to elicit physics.]

Let me also now demonstrate that $u_{out} \sim V_A$.

$$\{\Phi, \nabla_\perp^2 \Phi\} \sim \{\psi, \nabla_\perp^2 \psi\}$$

$$\partial_x \Phi (\partial_x^2 + \partial_y^2) \partial_y \Phi - \partial_y \Phi (\partial_x^2 + \partial_y^2) \partial_x \Phi$$

$$= u_y (\partial_x \partial_y u_y + \partial_y^2 \underbrace{\cancel{u_x}}_{0}) + \underbrace{\cancel{u_x}}_{0} (\partial_x^2 + \partial_y^2) u_y$$

because $u_x = 0$ along $x = 0$ (we are looking at the outflow from the sheet)

$$\partial_x \psi (\partial_x^2 + \partial_y^2) \partial_y \psi - \partial_y \psi (\partial_x^2 + \partial_y^2) \partial_x \psi$$

$$= -\underbrace{\cancel{B_y}}_{0} (\partial_x^2 + \partial_y^2) B_x + B_x (\partial_x^2 B_y + \partial_y^2 \underbrace{\cancel{B_y}}_{0})$$

because $B_y = 0$ on the $x = 0$ line

$$u_y \partial_x \partial_y u_y \sim B_x \partial_x^2 B_y \qquad \partial_x^2 B_y \sim \frac{V_A}{\delta^2}$$

incoming field

$$\frac{u_{out}^2}{\delta L} \sim \frac{B_x V_A}{\delta^2} \qquad (162e)$$

But $\nabla \cdot \vec{B} = 0$, so

$$\frac{B_x}{\delta} \sim \frac{V_A}{L} \qquad (162f)$$

We get therefore $\boxed{u_{out} \sim V_A}$ (162g)

The "<u>reconnection rate</u>" is

$$\frac{\partial \psi}{\partial t} \sim u_{in} V_A \sim \frac{\delta}{L} u_{out} V_A \sim S_L^{-1/2} V_A^2 \qquad (162h)$$

(the rate of change of flux at $x = 0 = y$, which is also $\propto$ electric field at that point)

This is the main result of the theory so far, due to Sweet (1958) & Parker (1957) [hereafter SP].

It translates into a characteristic reconnection time (time over which a large ~~an~~ fraction of magnetic flux that has come into the X-point configuration has been processed):

$$\tau_{SP} \sim \frac{L}{u_{in}} \sim \tau_A \sqrt{S_L}\ , \quad \tau_A = \frac{L}{V_A} \quad \text{Alfvén time} \qquad (162i)$$

Compare this to ordinary ohmic diffusion time of the magnetic field (on large scales):

$$\tau_\eta \sim \frac{L^2}{\eta} \sim \frac{L}{V_A}\frac{V_A L}{\eta} \sim \tau_A S_L \qquad (162j)$$

$$\gg \tau_{SP}$$

So, the nonlinearity, which is inherent in the reconnection process (because Lorentz force participates by setting up outflows), has accelerated things.

It has not, alas, accelerated them enough.

In a solar flare, the numbers are (Kelsrud's book § 14.4):

$S \sim 3\cdot 10^{12}$

$\tau_A \sim 40$ sec

$\tau_{SP} \sim 7\cdot 10^{7}$ sec (~ 2 yrs)

$\tau_\eta \sim 10^{14}$ sec ($\sim 10^{6}$ yrs) whereas observed energy release times for flares are in the range from 15 min ($\sim 10^3$ sec) to several hours ($\sim 10^4$ sec).

So SP reconnection is ~ 1000 times too slow (and similar discrepancies exist in other observable contexts, e.g., in the Earth's magnetotail).

The basic problem is intuitive: the long and thin current sheet, with resistively controlled aspect ratio, is the bottleneck. To process reconnected flux, you need also to process a mass flow — and the nozzle is too thin!

Thus was born the problem of "<u>fast reconnection</u>" and how to achieve/explain it.

- Microphysics not MHD? So sheet's width is determined by some other physics?
  But it's still <u>micro</u> physics, and at macroscales, MHD is fine, so X-point will collapse volens nolens!
- Somehow, the X-point collapse cannot be completed all the way to SP sheet?

Let us go back to the UL solution and consider it <u>before</u> (162a) aspect ratio is reached.

NB: In small enough systems, SP reconnection works fine! — indeed it was experimentally achieved on the MRX experiment in Princeton.

You might have imagined that everything was solved and nothing interesting (would) happen until the sheet collapsed to resistive width, but don't be too sure!

Imagine that the collapse process is happening at some finite rate: $\Gamma \sim \frac{u_0}{L_0}$ to start with and then, as in UL solution, slowing down as it goes along, $\Gamma \sim \frac{u_0}{L} \to 0$.

Consider therefore this simple solution to be instantaneously steady and ask whether it is stable, i.e., (in)vulnerable to much faster-growing perturbations. We are indeed going to discover that it is unstable.

4.2 Tearing Mode

NB: My exposition thus far and in what follows is a somewhat more pedagogical and updated version of Ap. D of my 2022 review of MHD turbulence (JPP).

4.2.1 Problem Set-Up

To deal with this question of stability of sheets (or, more precisely, collapsing X-points), let us distill a simple problem. We perturb the solution (156–157) so:

$$\Phi = \Phi_0 + \phi e^{\gamma t}, \quad \Psi = \Psi_0 + \psi e^{\gamma t}, \qquad (163)$$

where we formally ask that $\gamma \gg \Gamma \sim \frac{u_0}{L}$,
so we can treat the ideal collapsing solution as quasi-steady.

Once I work out γ, I can check a posteriori if it is indeed $\gg \Gamma$ — in fact, at that point I will ask what happens at the moment when γ gets to be comparable to Γ (the sheet will break up and its subsequent evolution will change).

A further simplification will be to assume that the collapse has gone on for some time, so $a \ll L$ and so all terms in (156-157) that involve $\frac{1}{L}$ are negligible, so, effectively,

$$\Phi_0 \simeq 0 \quad \text{and} \quad \Psi_0 \simeq \frac{v_A x^2}{2a} \qquad (164)$$

This makes one think of a case of no ep-in flow and $B_0(x) = \frac{v_A}{a} x \hat{y}$ (165)

This is, in fact, a little awkward, as we shall see shortly, and it would seem more physical to consider instead a generic profile $B_0(x)$ that flattens out at $x \to \pm\infty$

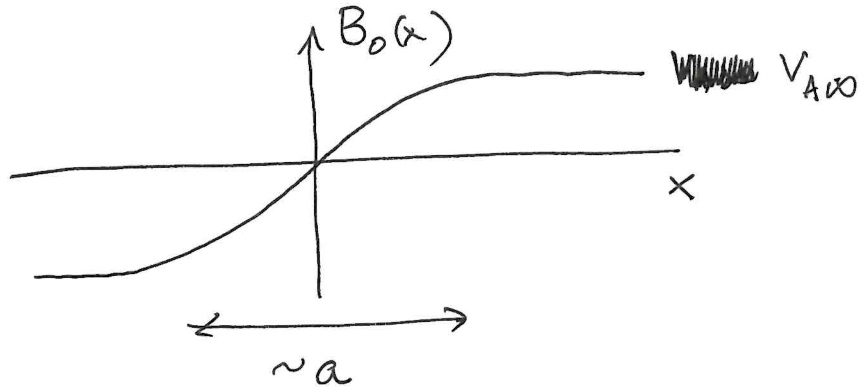

So, we are looking at stability at

$x \sim a \ll L$ and $y \ll L$ (where flows are small)

That finally gives us our super-simplified set-up:

$$\Phi = \phi(x,y)e^{\gamma t}, \quad \Psi = \Psi_0(x) + \psi(x,y)e^{\gamma t}$$

$$\vec{B} = \hat{y}\,\underbrace{\Psi_0'(x)}_{\equiv B_0(x)} + \hat{z}\times\nabla\psi\, e^{\gamma t} \tag{166}$$

this can be $\delta\vec{B}_\perp$ because a strong field in the $\hat{z}$ direction is allowed, as long as $\frac{\partial}{\partial z}$ is negligible everywhere

You might think this is far too simplified, and so do many other people – there are a 1001 papers generalising the calculation that I am about to do to various set ups with some of the simplifying assumptions relaxed – after you know how to do the simple thing, you can explore and enjoy (or even contribute).

Since only x is the only inhomogeneous direction now, we can Fourier-transform in y.

Substitution of (166) into (154-155) gives us

$$\begin{cases} \gamma(\partial_x^2 - k_y^2)\phi = \psi_0'(x)\, ik_y(\partial_x^2 - k_y^2)\psi - \psi_0'''(x)\, ik_y\psi \\ \qquad = ik_y\left[B_0(x)(\partial_x^2 - k_y^2) - B_0''(x)\right]\psi & (167) \\ \left[\gamma - \eta(\partial_x^2 - k_y^2)\right]\psi = ik_y B_0(x)\phi & (168) \end{cases}$$

This is a problem with a boundary layer if η is small. The (inverse) time scales involved are, a priori,

$$\underbrace{\tau_\eta^{-1} \equiv \frac{\eta}{a^2}}_{\text{resistive}} \sim k_y^2\eta \ll \underbrace{\gamma}_{\substack{\text{intermediate} \\ \text{(by assumption!)}}} \ll \underbrace{k_y B_0 \sim \frac{v_A}{a} \equiv \tau_A^{-1}}_{\text{ideal (Alfvénic)}} \qquad (169)$$

scale of variation in x

4.2.2 Outer Region

This is only true in the "outer region" (by definition)

Let us solve there and discover that that is not enough.

In (167), the lhs is negligible, so

$$\partial_x^2 \psi = \left[k_y^2 + \frac{B_0''(x)}{B_0(x)}\right]\psi \qquad (170)$$

magnetic force balance

In (168), the η term is negligible:

$$\gamma \psi = i k_y B_0(x) \phi \qquad (171)$$

magnetic perturbation arising from advection of eq-m field by perturbed flow

So, solving for ϕ is trivial, but for ψ we need to solve an ODE.

To solve it, there are two possible strategies. One obvious one is to assume some specific function $B_0(x)$ ~~and~~ conveniently chosen to make (170) analytically solvable. The most classic such choice is the "Harris (1962) sheet"

$$B_0(x) = v_A \tanh\frac{x}{a} \qquad (172)$$

This is what is treated in most textbooks.

I am, however, partial to a different approach, in whose development I have ~~[illegible]~~ had some involvement (Loureiro et al. 2007) and which I therefore ~~[illegible]~~, unsurprisingly, find more physically appealing.

Let us make a further assumption:

$$k_y a \ll 1 \qquad (173)$$

(perturbations are longer than the sheet is wide).
We will see a posteriori that this is OK.

Eq. (170) simplifies:

$$\partial_x^2 \psi = \frac{B_0''(x)}{B_0(x)} \psi \qquad (174)$$

and becomes solvable in the form

$$\psi = B_0(x)\,\chi(x) \qquad (175)$$

because $B_0(x)$ is a solution

$$\partial_x \psi = B_0'(x)\chi + B_0(x)\chi'$$

$$\partial_x^2 \psi = B_0''(x)\chi + 2B_0'(x)\chi' + B_0(x)\chi''$$

$$B_0(x)\chi'' + 2B_0'(x)\chi' = 0$$

$$\frac{\chi''}{\chi'} = -2\frac{B_0'}{B_0} \Rightarrow \chi' = C_1 \frac{1}{B_0^2(x)}$$

$$\Rightarrow \chi = C_2 + C_1 \int_{x_0}^{x} \frac{dx'}{B_0^2(x')}$$

x_0 somewhere (does not matter where because any difference absorbable into C_2)

Thus,

$$\psi = B_0(x)\left[C_2^{\pm} + C_1^{\pm}\int_{\pm x_0}^{x} \frac{dx'}{B_0^2(x')}\right] \qquad (176)$$

$\pm$ here corresponds to solutions at $x>0$ and $x<0$
(my integral is from outside inwards, but not crossing $x=0$ because there is boundary layer lurking there).

$B_0(x)$ is an odd function, so let us assume

$$B_0(x) \approx \frac{V_A}{a} x \quad \text{as } x \to 0 \qquad (177)$$

The integral in (176) will then be dominated by the upper limit, with everything else a negligible constant:

$$\psi \approx \frac{V_A}{a} x \left[C_2^{\pm} + C_1^{\pm} \left(-\frac{a^2}{V_A^2} \frac{1}{x} + \dots \right) \right]$$

$$= -\frac{a}{V_A} C_1^{\pm} + \dots \Rightarrow \quad C_1^{\pm} = -\frac{V_A}{a} \psi(0) \qquad (178)$$

a single constant

Now consider what ψ does as $x \to \infty$ ($\gg a$).

Let us assume that

can be $= V_A$, but doesn't have to be

$$B_0(x) \to \pm V_{A,\infty} = \text{const} \qquad (179)$$

(like in Harris sheet). Then

$$\psi \approx \pm V_{A,\infty} \left[C_2^{\pm} - \frac{V_A}{a} \psi(0) \left(\frac{x}{V_{A\infty}^2} + f(x_0) \right) \right] \qquad (180)$$

some constant that depends on x_0 and the shape of $B_0(x)$

$$= \pm V_{A,\infty} \left[C_2^{\pm} - \frac{V_A}{a} \psi(0) f(x_0) \right]$$

$$\mp \frac{V_A}{V_{A,\infty}} \psi(0) \frac{x}{a}$$

But wait, if we assumed (179), that means

$$\frac{B_0''(x)}{B_0(x)} \to 0 \quad \text{as } x \to \pm\infty,$$

So in fact we cannot have neglected

$$k_y^2 \ll \frac{B_0''(x)}{B_0(x)}$$

at large x. Let us see what the solution is in the opposite limit, when k_y is dominant:

$$\partial_x^2 \psi = k_y^2 \psi$$

$$\hookrightarrow \psi = C_3^{\pm} e^{\mp |k_y| x} \qquad (181)$$

making sure that $\psi \to 0$ at $x \to \pm\infty$

At $k_y x \to 0$, this is

$$\psi \approx C_3^{\pm}(1 \mp |k_y| x) \qquad (182)$$

Let us then match this with (180):

$$C_3^{\pm} |k_y| = \frac{V_A}{V_{A\infty}} \psi(0) \frac{1}{a} \iff C_3^{\pm} = \frac{V_A}{V_{A\infty}} \frac{\psi(0)}{|k_y| a}$$

$$\text{and} \quad C_3^{\pm} = \pm V_{A\infty} \left[C_2^{\pm} - \frac{V_A}{a} \psi(0) f(x_0) \right] \qquad (183)$$

$$\hookrightarrow C_2^{\pm} = \frac{V_A}{a} \psi(0) f(x_0) \pm \frac{V_A}{V_{A\infty}^2} \frac{\psi(0)}{|k_y| a} \qquad (184)$$

This tells us now everything we need to know about the solution at $x \to 0$:

$$\psi = B_0(x) \frac{V_A}{a} \psi(0) \left[f(x_0) \pm \frac{1}{|k_y| V_{A\infty}^2} - \int_{\pm x_0}^{x} \frac{dx'}{B_0^2(x')} \right] \qquad (185)$$

and $$\psi = \frac{V_A}{V_{A\infty}} \frac{\psi(0)}{|k_y|a} e^{\mp|k_y|x} \quad \text{as } x \to \pm\infty \qquad (186)$$

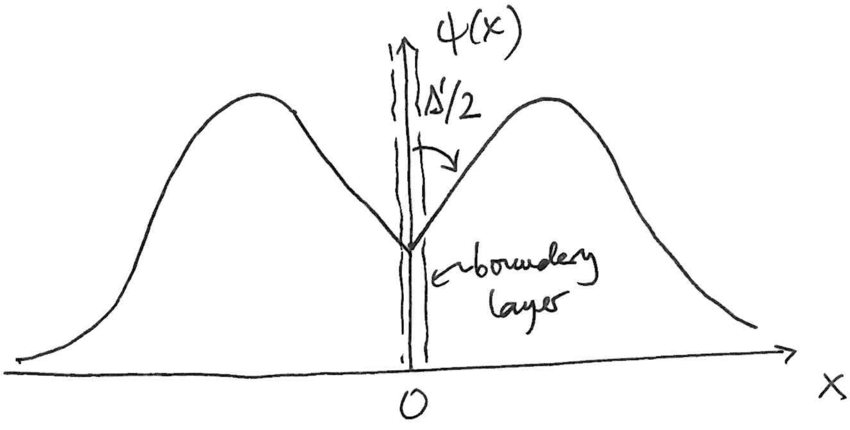

The derivative at O is discontinuous. In fact it was perhaps obvious that that should have happened because $\psi(x)$ is an even function and the magnetic field must reverse direction at $x=0$ — that corresponds to a singular current developing there, about to be resolved by resistivity. This discontinuity is measured by

$$\boxed{\Delta' \equiv \frac{\partial_x\psi(+0) - \partial_x\psi(-0)}{\psi(0)} \underset{\substack{\uparrow \\ \text{using} \\ B_0(x) \approx \frac{V_A}{a}x}}{=} 2\left(\frac{V_A}{V_{A\infty}}\right)^2 \frac{1}{|k_y|a^2}} \qquad (187)$$

The key interesting dependence here is $\Delta' a \propto (|k_y|a)^{-1}$. This is not a universal result: you can invent profiles of $B_0(x)$ for which it is different, e.g., $\Delta' a \propto (|k_y|a)^{-2}$ for $B_0(x) = V_A \sin\frac{x}{a}$ (Boldyrev & Loureiro 2018) but the scaling in (187) <u>is</u> universal if you assume that $B_0(x) \to \pm V_{A\infty} = \text{const}$ as $x \gg a$, rather than $B_0(x) \to 0$ on the scale $x \sim a$.

Below, I will do everything for (187), but it is easily generalizable for any other scaling of Δ'.

Why do I need to know Δ'? Because that will be the parameter to which I will have to match the inner solution in the boundary layer and on which ultimately the (iii) stability will depend — Δ' play the role of the "drive" parameter.

4.2.3 Inner Region

This region will have in x some width

$$\partial_x^{-1} \sim \delta_{in} \ll a,\ k_y^{-1}$$

and will have some scaling with η, which is not as yet obvious, but is tbd.

Let us see what eqns (167–168) become there:

keeping ∂_x terms only!

$$\begin{cases} \gamma \partial_x^2 \phi = i k_y B_0(x) \partial_x^2 \psi \\ \qquad \approx i k_y v_A \dfrac{x}{a} \partial_x^2 \psi & (188) \\ (\gamma - \eta \partial_x^2) \psi \approx i k_y v_A \dfrac{x}{a} \phi & (189) \end{cases}$$

Let us turn these into a single equation:

$$\partial_x^2 \psi \underset{(188)}{=} -i \frac{\gamma a}{k_y v_A} \frac{1}{x} \partial_x^2 \phi \underset{(189)}{=} -\left(\frac{\gamma a}{k_y v_A}\right)^2 \frac{1}{x} \partial_x^2 \frac{1}{x}\left(1 - \frac{\eta}{\gamma}\partial_x^2\right)\psi \qquad (190)$$

You can now instantly read off the width of the boundary layer from here because it is basically whatever it needs to be to make the term with the highest derivative non-small:

$$\left(\frac{\gamma a}{k_y v_A}\right)^2 \frac{\eta}{\gamma} = \delta_{in}^4 \qquad (191)$$

Let us therefore rescale $x = X\delta_{in}$:

$$\partial_X^2 \psi_{in} = -\frac{1}{X}\partial_X^2 \frac{1}{X}\left(\Lambda - \partial_X^2\right)\psi_{in} \qquad (192)$$

where $\psi_{in}(X) = \psi(X\delta_{in})$ and

$$\Lambda = \left(\frac{\gamma a}{k_y v_A}\right)^2 \frac{1}{\delta_{in}^2} \qquad (193)$$

from (191)

$$\frac{\gamma \delta_{in}^2}{\eta} = \frac{\text{growth rate}}{\text{res. rate}}$$

This is an eigenvalue problem for Λ (no other parameters here!) and if we can solve (192), we then find Λ by matching the solution to (187), like so:

$$\Delta' = \frac{2}{\delta_{in}} \int_0^\infty dX \, \frac{\partial_X^2 \psi_{in}(X)}{\psi_{in}(0)} \qquad (194)$$

This condition will lead to an equation of the form

$$\Delta'\delta_{in} = f(\Lambda) \qquad (195)$$

function that depends on nothing but Λ

$$\frac{\delta_{in}}{a} = \left(\frac{\gamma\eta}{V_A^2}\right)^{1/4}\frac{1}{\sqrt{k_y a}} \text{ from (191) } = \left(\frac{\gamma\tau_A}{S_a}\right)^{1/4}\frac{1}{\sqrt{k_y a}} \qquad (196)$$

It is going to be useful to have γ in terms of Λ everywhere: from (193),

$$\Lambda = \left(\frac{\gamma a}{k_y V_A}\right)^2 \cdot \sqrt{\frac{\gamma}{\eta}}\,\frac{k_y V_A}{\gamma a} = \frac{\gamma^{3/2} a}{k_y V_A \eta^{1/2}} = \frac{\gamma^{3/2} a^2}{k_y a V_A \eta^{1/2}}$$

$$= \frac{(\gamma\tau_A)^{3/2}}{k_y a} S_a^{1/2}, \text{ where } \tau_A = \frac{a}{V_A} \text{ and } S_a = \frac{V_A a}{\eta} \qquad (197)$$

τ_A: Alfvén time based on a

S_a: Lundquist number based on a

$\Downarrow$

$$\gamma\tau_A = \Lambda^{2/3}(k_y a)^{2/3} S_a^{-1/3} \qquad (198)$$

$$\frac{\delta_{in}}{a} = \Lambda^{1/6}(k_y a)^{1/6-1/2} S_a^{-1/12-1/4} = \Lambda^{1/6}(k_y a)^{-\frac{1}{3}} S_a^{-\frac{1}{3}} \qquad (199)$$

So (195) becomes

$$\frac{f(\Lambda)}{\Lambda^{1/6}} = \Delta' a\,(k_y a S_a)^{-1/3} \overset{(187)}{=} 2\left(\frac{V_A}{V_{A\infty}}\right)^2\left[(k_y a)^4 S_a\right]^{-\frac{1}{3}} \qquad (200)$$

find Λ from (195) $\Rightarrow$ get γ and k_y

To solve for Λ and, therefore, for γ, we need $f(\Lambda)$ and so ψ_{in} (X).

4.2.5 Fastest tearing

Solving eqn. (192) for δ_{in} exactly is a task that is applied-mathematically worthwhile and has been done in a number of ways in a number of papers – Boldyrev & Loureiro 2018 is a modern review, featuring a new method.

But we can be lazy and get to the answer cheaply. Since $f(\Lambda)$ depends on nothing but Λ and both are dimensionless, it is an easy guess that the peak growth of the mode should occur at

$$\Lambda \sim 1 \quad \text{and} \quad f(\Lambda) \sim 1 \tag{201}$$

If that is true, then

$$(200) \to \quad k_y a \sim S_a^{-1/4} \equiv k_* a \tag{202}$$

$$(198) \to \quad \boxed{\gamma \tau_A \sim S_a^{-1/2}} \tag{203}$$

$$(199) \to \quad \frac{\delta_{in}}{a} \sim S_a^{-1/4} \tag{204}$$

NB: $\ll 1$, so it was indeed OK to assume this in (173)

NB: In order for this solution to be realizable, it has to fit into the sheet, i.e.,

$$k_* L \gtrsim 1 \iff \frac{L}{a} \gtrsim S_a^{1/4} = S_L^{1/4}\left(\frac{a}{L}\right)^{1/4} \tag{205}$$

$$\iff \frac{L}{a} \gtrsim S_L^{1/5}$$

this is still in the "ideal" regime vis-à-vis condition (162a)

We can also check, immediately, ~~[illegible]~~ how the growth rate (203) compares to the rate at which the X-point collapse occurs:

$$\frac{\gamma}{u_0/L} \sim \frac{L}{a}\gamma\tau_A \sim \frac{L}{a} S_a^{-1/2} \sim \left(\frac{L}{a}\right)^{3/2} S_L^{-1/2} \gtrsim 1$$

$u_0 \sim v_A$

if $\boxed{\frac{L}{a} \gtrsim S_L^{1/3}}$ (206)

This too happens before an SP sheet is formed. This was proposed by Pucci & Velli (2014) to be the largest possible aspect ratio to which a sheet could collapse — what happens after that depends on how the tearing mode saturates. They called this tearing mode "ideal tearing" because in sheet (206), the tearing growth rate is ~~[illegible]~~ independent of η.

I will discuss the nonlinear evolution of the tearing mode shortly, but first I want to show you that (201) was reasonable and also what wd happen if the fastest-growing mode does not fit into the sheet, i.e., (205) is not satisfied.

4.2.7 FKR Solution

Suppose $\Lambda \ll 1$.

Recall (193): $\Lambda = \dfrac{\gamma \delta_{in}^2}{\eta} = \dfrac{\gamma}{\text{Ohmic diff. rate}}$ "slow" growth.

Let's Taylor-expand

$$f(\Lambda) \sim \Lambda \qquad (207)$$

(I am not proving it here, but it is plausible!)

$$(200) \to \Lambda^{5/6} \sim (k_y a)^{-4/3} \delta_a^{-1/3}$$

$$\Lambda \sim (k_y a)^{-8/5} \delta_a^{-2/5} \qquad (208)$$

$$(198) \to \boxed{\gamma \tau_A \sim (k_y a)^{-2/5} \delta_a^{-3/5}} \qquad (209)$$

$k_y a \gg \delta_a^{1/4} \sim k_* a$ to ensure $\Lambda \ll 1$

$$(187) \to \Delta' a \sim \frac{1}{k_y a} \ll \delta_a^{-1/4}, \qquad (210)$$

which is why this is called the "small-Δ'" (or weakly driven) limit

This was the first kind of tearing mode to get solved (exactly), by Firth, Kileen & Rosenbluth (1963) — the solution is known as FKR solution, and that is what you will find worked out carefully in most textbooks.

NB $(199) \to \dfrac{\delta_{in}}{a} \sim \Lambda^{1/6} (k_y a)^{-1/3} \delta_a^{-1/3}$

$$\sim (k_y a)^{-\frac{4}{15}-\frac{1}{3}} \delta_a^{-\frac{1}{15}-\frac{1}{3}} \sim (k_y a)^{-\frac{3}{5}} \delta_a^{-\frac{2}{5}} \qquad (208a)$$

For completeness, let me show you how to do this.
The trick is actually, rather than combining (188) & (189) into a single eqn (190) for ψ, to combine them into an equation for ϕ:

$$(\gamma - \eta\partial_x^2)\psi = i k_y v_A \frac{x}{a}\phi \qquad (189)$$

$$\partial_x^2 \psi = -i \frac{a\gamma}{k_y v_A x}\partial_x^2 \phi \qquad (188)$$

$$\gamma\psi + i\frac{a\gamma\eta}{k_y v_A x}\partial_x^2\phi = i k_y v_A \frac{x}{a}\phi \qquad (210a)$$

assume a priori (to discover a posteriori that this is OK) that $\gamma \ll \eta\partial_x^2$ — Ohmic diffusion rate across the layer is fast. Then we can expand

meaning $\Lambda \ll 1$

$$\psi(x) \approx \psi(0) + \dots$$

This is called the "<u>constant-ψ approximation</u>".

Then, from (210a)

$$1 + i\frac{a\cancel{\gamma}\eta}{k_y v_A \psi(0)}\frac{1}{x}\partial_x^2\phi = i\frac{k_y v_A}{a\gamma\psi(0)} x\phi \qquad (210b)$$

Let $x = X\delta_{in}$:

$$1 + i\frac{a\cancel{\gamma}\eta}{k_y v_A\psi(0)\delta_{in}^3}\frac{1}{X}\partial_X^2\phi = i\frac{k_y v_A \delta_{in}}{a\gamma\psi(0)} X\phi$$

$$\equiv -\lambda(X)$$

$$1 + X\chi = \cancel{-i}\,\frac{a\eta}{k_y v_A \cancel{\psi(0)}\,\delta_{in}^3}\,\frac{1}{X}\,\partial_X^2\,\frac{\chi}{\cancel{-i}\,\dfrac{k_y v_A \delta_{in}}{a\gamma\,\cancel{\psi(0)}}}$$

$$= \frac{a^2\gamma\eta}{(k_y v_A)^2\,\delta_{in}^4}\,\frac{1}{X}\,\partial_X^2\chi\,,$$

So

define δ_{in} so that this is 1

$$\delta_{in} = (\gamma\eta)^{1/4}\left(\frac{a}{k_y v_A}\right)^{1/2} \qquad (210c)$$

$$\boxed{\partial_X^2\chi = X(1+\chi X)} \qquad (210d)$$

This equation has no parameters at all. Let us imagine we have solved it. In fact, no need to imagine, there is a solution that is called the Rutherford–Furth solution:

$$\chi(X) = -\frac{X}{2}\int_0^1 d\mu\, e^{-\frac{1}{2}\mu X^2}(1-\mu^2)^{-1/4} \qquad (210e)$$

You can substitute and check that it works. But the important thing is simply that it's true, because now we can calculate everything from fixing Δ' according to (187), or (194):

$$\Delta' = \frac{2}{\delta_{in}}\int_0^\infty dX\,\frac{\partial_X^2\psi_{in}}{\psi_{in}(0)}$$ where δ_{in} is (210c)

Let us work this out in terms of $\chi(X)$.

$$\frac{\partial_X^2\psi_{in}}{\psi_{in}(0)} = \frac{\delta_{in}^2}{\psi(0)}\,\partial_x\psi \underset{(188)}{=} \frac{\delta_{in}^3}{\psi(0)}\left(-i\,\frac{a\gamma}{k_y v_A X}\right)\partial_x^2\phi$$

$$\underset{\text{def. of }\alpha}{=} \frac{1}{\delta_{in}}\left(\cancel{-i}\,\frac{a\gamma}{k_y v_A\,\cancel{\psi(0)}}\right)\frac{1}{X}\,\partial_X^2\,\frac{\alpha}{\dfrac{\cancel{-i}\,k_y v_A\delta_{in}}{a\gamma\,\cancel{\psi(0)}}}$$

$$= \frac{a^2\gamma^2}{(k_y v_A)^2\delta_{in}^2}\,\frac{\partial_X^2\alpha}{X} \underset{(210d)}{=} \left(\frac{a\gamma}{k_y v_A}\right)^2\frac{1}{\delta_{in}^2}\,(1+\alpha X), \qquad (210f)$$

whence

$$\Delta' = \left(\frac{a\gamma}{k_y v_A}\right)^2\frac{1}{\delta_{in}^3}\,\underbrace{2\int_0^\infty dX\,(1+\alpha X)}_{\text{use }(210e)} \qquad (210g)$$

So we have, using (210e),

$$\underbrace{2\int_0^\infty dX\,(1+\alpha X)}_{\text{use }(210e)} = \pi\,\frac{\Gamma(3/4)}{\Gamma(1/4)}, \text{ as it happens}$$

$= I$ important thing is that it is a number!

$$\left(\frac{a}{k_y v_A}\right)^2\gamma^2(\gamma\eta)^{-3/4}\left(\frac{a}{k_y v_A}\right)^{-3/2} I = \Delta' \qquad (210h)$$

$$\gamma^{\frac{5}{4}}\,\eta^{-\frac{3}{4}}\left(\frac{a}{k_y v_A}\right)^{\frac{1}{2}} I = \Delta' \underset{(187)}{=} 2\left(\frac{v_A}{v_{x0}}\right)^2\frac{1}{|k_y|a^2}$$

$$\gamma \overset{a/v_A}{\tau_A} = \eta^{\frac{3}{5}}\left(\frac{a}{k_y v_A}\right)^{-\frac{2}{5}} I^{-\frac{4}{5}}\left[2\left(\frac{v_A}{v_{x0}}\right)^2\right]^{\frac{4}{5}}\frac{a}{v_A}\,k_y^{-4/5}a^{-}$$

$$= \left[\frac{2}{I}\left(\frac{v_A}{v_{x0}}\right)^2\right]^{\frac{4}{5}} S_a^{-3/5}\,(k_y a)^{-2/5} \qquad (210i)$$

If you like, this is the derivation of (207)!

— Same as the educated guess (209)!

4.2.8 Coppi Solution

Naturally, as one does, let us consider the opposite limit. Contrary to what you might have imagined, that is not $\Lambda \gg 1$ — it's not reasonable to expect a mode to grow at $\gamma \gg$ Ohmic diffusion rate inside the inner layer (otherwise there wd not be an inner layer!). So $\Lambda \sim 1$ is likely the limit of how large Λ can be, but what if $\Delta' a$ is large?

This corresponds to

in fact, it turns out, $\Lambda \to 1-0$

$$\Lambda \sim 1, \quad f(\Lambda) \to \infty \tag{211}$$

Then (198) $\to$ $\boxed{\gamma \tau_A \sim (k_y a)^{2/3} S_a^{-1/3}}$ (212)

$$(199) \to \quad \frac{\delta_{in}}{a} \sim (k_y a)^{-1/3} S_a^{-1/3} \tag{213}$$

$$(200) \to \quad f(\Lambda) \sim (k_y a)^{-4/3} S_a^{-1/3} \gg 1 \tag{214}$$

provided $k_y a \ll S_a^{-1/4} \sim k_* a$

This limit too has been solved exactly, by Coppi et al. (1976) — the "Coppi mode"

4.2.9 Tearing dispersion relation

So we are now in a position to sketch the tearing mode's dispersion relation and confirm that (212) is the ascending asymptotic at $k_y \ll k_*$, (209) the descending one at $k_y \gg k_*$ and they meet at k_* to give the max. growth rate (203), as anticipated

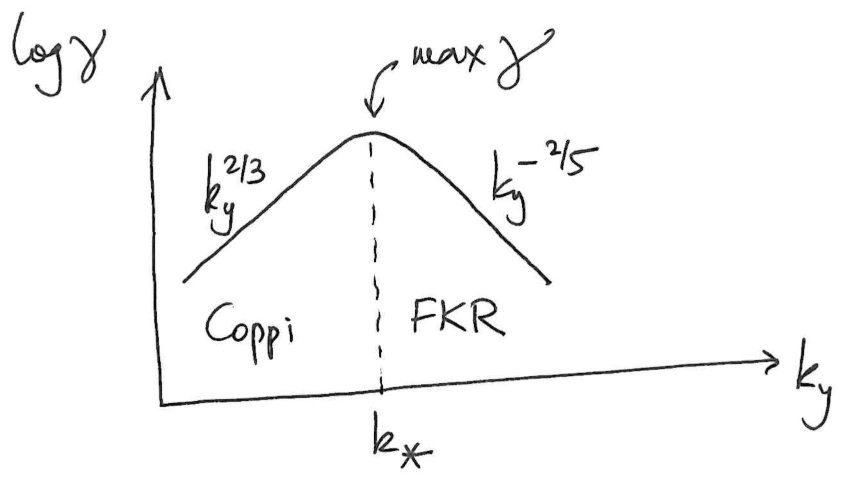

We can, finally, ask the question of whether, on account of the sheet being too short, either Coppi or FKR mode might disrupt it earlier than the max.-growth one can.
The answer is obviously no: shorter L means larger minimum k_y, pushing the system into the FKR regime, with $\gamma \ll \gamma_{max}$. That smaller γ will not get to rival Γ earlier than γ_{max} does and by the time γ_{max} does, it will be able to, because condition (205) will have been amply satisfied.

If you want a full derivation of the Coppi solution, see Coppi's paper or Boldyrev & Loureiro (2018).

4.4 Nonlinear ~~[illegible]~~ evolution of the tearing mode

What does tearing mode look like?

Recall (166):

$$\psi = \psi_0(x) + \psi(x,y)\, e^{\gamma t}$$
$$= \psi_0(x) + \psi(x) \cos k_y y\, e^{\gamma t}$$

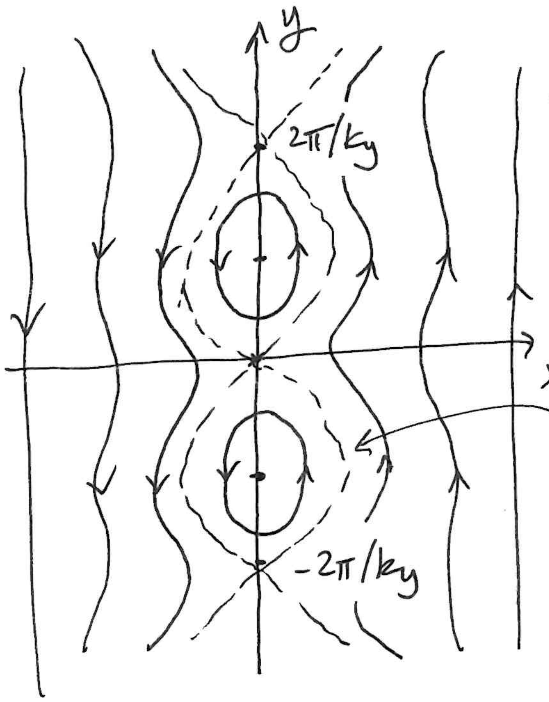

unperturbed field (collapsing sheet)

island width

$$e^{\gamma t}\psi(0) = \underbrace{\psi_0\left(\tfrac{W}{2}\right)}_{\simeq\ \frac{1}{2}\underbrace{\psi_0''(0)}_{=\ \frac{V_A}{a}}\frac{W^2}{4}} - \underbrace{\psi\left(\tfrac{W}{2}\right)}_{\simeq\ \psi(0)} e^{\gamma t}$$

(only true in FKR regime, but ok on "$\sim$" level)

a chain of islands

So, $$W \sim \left(\frac{a\psi}{V_A}\right)^{1/2} \sim \left(\frac{a}{V_A}\frac{\delta B_x}{k_y}\right)^{1/2} \qquad (215)$$

Another way to see this is to say that the typical angular distortion of a field line is

$$W k_y \sim \frac{\delta B_x}{B_0(W)} \sim \frac{\delta B_x}{\frac{V_A}{a} W} \qquad (216)$$

Note that then

$$\underset{\uparrow \text{ solenoidality}}{\delta B_y \sim \frac{\delta B_x}{W k_y}} \sim \frac{W}{a} V_A\text{, i.e., at } x\sim W,\ \delta B_y \sim B_0(W). \qquad (216a)$$

Generally speaking, the tearing mode will go nonlinear once the islands of the perturbation no longer fit inside the inner layer:

$$w \sim \delta_{in} \qquad (217)$$

If $\delta_{in}\Delta' \ll 1$ (FKR), one can show that linear growth will be replaced by secular growth (Rutherford 1973), which will continue until

$$w \sim (\Delta')^{-1} \qquad (218)$$

~~[illegible]~~
(Militello & Porcelli 2004, Escande & Ottaviani 2004).
This, however is not a specially interesting regime for us as we are expecting our collapsing sheet to go unstable to the fastest-growing tearing mode first, and for it,

$$\Delta' \sim \frac{1}{k_y a^2} \underset{(202)}{\sim} S_a^{1/4}\frac{1}{a} \underset{(204)}{\sim} \frac{1}{\delta_{in}}, \qquad (219)$$

So there is no space for the secular regime.
What kind of nonlinear evolution do we then expect? Let us see what is the size of all the fields when (217) is satisfied.

From (216), $$\delta B_x \sim v_A \frac{w^2}{a} k_y \qquad (220)$$
$$\sim v_A \frac{\delta_{in}^2}{a} k_y$$

Then, from solenoidality, (216a)

$$\delta B_y \sim v_A \frac{w}{a} \sim v_A \frac{\delta_{in}}{a} \quad (221)$$

From (188), in a tearing mode,

$$\delta u_y = \partial_x \phi \sim \frac{k_y v_A}{\gamma a} x \partial_x \psi \sim \frac{k_y v_A}{\gamma a} \delta_{in} \delta B_y \quad (222)$$

$$\sim \delta B_y\,!$$

But this is just telling us that an

$$\frac{k_y a}{\gamma \tau_A} \frac{\delta_{in}}{a} \sim \frac{S_a^{-1/4}}{S_a^{-1/2}} S_a^{-1/4} \sim 1$$

Alfvénic outflow has been formed. We also see immediately that the rate at which this outflow is (nonlinearly) evolving our perturbation is

$$k_y \delta u_y \sim k_y v_A \frac{\delta_{in}}{a} \sim S_a^{-1/2} \sim \gamma, \quad (223)$$

so it is indeed competitive with the tearing mode. This is not surprising at all. What our tearing calculation has shown us is that an ideally collapsing sheet will develop a chain of islands on top of it, separated by mini-X-points. And what we now see is that once these islands grow large enough, their dynamics will be once again Alfvénic (so ideal) — and we already know that this means that ~~they will[illegible]~~ the

They do! [see Loureiro et al 2005]

X-point between them will want to collapse! ~~[illegible]~~ So the saturation of tearing will be due to the very same physics that ~~[illegible]~~ triggered it in the first place, but now on smaller scales, with the new length of the sheet starting at $\sim k_y^{-1}$.

4.4.1 Recursive Tearing

It is not hard to imagine subsequent dynamics:

these X-points will start collapsing, will in turn become unstable to ("secondary") tearing and so on, giving rise to a hierarchy of island chains.

There are some uncertainties about exactly how to set this up — I will not go into this here, but recommend to you §D.5.2 of my MHD turbulence review for a summary of schemes proposed so far (including my own). None of this probably matters. What does matter is that collapsing sheets break out into a multitudes of islands (called "plasmoids" in this context) of different sizes. Because all of this now lives ~~[illegible]~~ in a world of not just reversing magnetic fields but also outflows from various sheets

relevant papers are Shibata & Tanuma (2001) and Tenerani et al. (2015).

(or collapsing X-points), the islands will move, encounter each other, merge (there is a coalescence instability, which again involves reconnection of the islands' fields — and can even create little sheets full of secondary islands oriented transversely to the main sheet — in the x direction), etc. Thus, a plasmoid chain.

4.5 Fast MHD reconnection

It is about to transpire that the rate at which this chain reconnects magnetic fields is independent of η, but first we must work out what the structure of the chain is.

For that, we will, perhaps unexpectedly, need to recall the SP sheet (§4.2). It might have seemed from the above discussion that such a sheet would never form because a collapsing UL solution wd go tearing-unstable already when (206) is satisfied:

$$\frac{L}{a} \gtrsim S_L^{1/3} \gg S_L^{1/2} \underbrace{\sim}_{\text{SP case (162d)}} \frac{L}{\delta} \qquad (206)$$

and after that there will be plasmoids galore.

This is true, but only asymptotically when $S_L \gg 1$.

In order for collapsing sheets to go unstable, in practice, the Lundquist number has to exceed a certain critical value that allows the tearing's inner layer to fit comfortably, and in a scale-separated way, inside the sheet. There is no rigorous theoretical calculation of this S_c, but it is quite easy to estimate non-rigorously.

4.5.1 Plasmoid Instability

Let us imagine an SP sheet has managed to form. It will then be subject to tearing that satisfies (202), (203) and (204) but with

$$a = \delta \sim L S_L^{-1/2} \qquad (224)$$

This gives

$$\gamma \sim \frac{v_A}{\delta} S_\delta^{-1/2} \sim \frac{v_A}{L} S_L^{-1/2}\left(\frac{\delta}{L}\right)^{-3/2} \sim \frac{v_A}{L} S_L^{1/4} \qquad (225)$$

$$k_y L \sim \frac{L}{\delta} S_\delta^{-1/4} \sim \left(\frac{\delta}{L}\right)^{-5/4} S_L^{-1/4} \sim S_L^{3/8} \qquad (226)$$

$$\frac{\delta_{in}}{\delta} \sim S_\delta^{-1/4} \sim S_L^{-1/4}\left(\frac{\delta}{L}\right)^{-1/4} \sim S_L^{-1/8} \qquad (227)$$

This instance of a tearing instability of an SP sheet is called the plasmoid instability, which entered the consciousness of the research community when Loureiro et al (2007) was published, even though it later turned out that Tajima & Shibata (1997) already had it but did not seem to realize the implications.

[Moral of the story: when you see low-hanging fruit, you need to realize not only that it is low-hanging, but that it is fruit!]

The immediate conclusion is that SP sheets are very violently unstable: $\gamma \gg V_A/L$, so much <u>faster</u> than the rate of dynamical evolution. This is as expected as the SP sheet is much thinner than the marginal sheet (206).

However, in order to be actually unstable, it has to have a large enough S_L that (227) gives a decent scale separation between δ_{in} and δ, i.e., what we need is

$$S_L^{1/8} \gg 1$$

Well, let us guess

$$\underset{\text{(at least)}}{S_L^{1/8} \gtrsim 3} \equiv S_c^{1/8} \Rightarrow \boxed{S_c \sim 10^4}. \quad (228)$$

Below this, SP sheets can survive quite happily — as they did, mostly, until ~mid-2000's, when computer simulations became large enough to resolve (228) (although, to be fair, already Biskamp 1986 saw a plasmoid — but again, people did not seem to have connected the dots).

4.5.2 Critical sheet

If we now invert the logic of these formulae, we may conclude that, given some S_L, the longest possible sheet that can be SP is

$$L_c \sim L \frac{S_c}{S_L} = \frac{S_c \eta}{V_A}, \qquad (229)$$

in which

$$\delta_c \sim L_c S_c^{-1/2} \text{ and rec. rate } \left(\frac{\partial \psi}{\partial t}\right)_c \sim S_c^{-1/2} V_A^2 \qquad (230)$$

Our plasmoid chain then must be composed of many plasmoids, all of different sizes, but separated by sheets $\sim L_c$ (if the sheet is stretched longer, it goes unstable; if it is shorter, it is still collapsing).

4.5.3 Scale-invariant reconnection

Consider all the plasmoids in a sheet to belong to many hirarchically nested levels, with (n+1)st-level plasmoids living in local sheets (in fact hirarchical chains) that connect nth-level ones. At every level, they are travelling with Alfvénic outflow, reconnecting the upstream field (the same at every level) and depositing the reconnected flux into n-th-level plasmoids

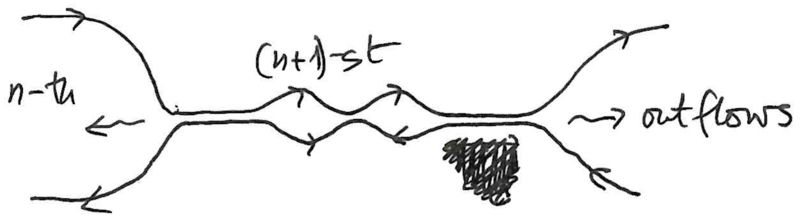

The reconnection rate at this n-th level is, by (162b):

$$\frac{\partial \psi^{(n)}}{\partial t} \sim \frac{\delta^{(n)}}{L^{(n)}} V_A^2 , \qquad (231)$$

where $L^{(n)}$ is the length of the sheet connecting n-th-level plasmoids and

$$\delta^{(n)} \sim w^{(n+1)} \qquad (232)$$

— the width of the (n+1)-st-level plasmoids.
This is the effective width because travelling plasmoids carry the required mass, as well as flux.
$w^{(n+1)}$ can be found if we assume that typically, in the nonlinear regime, the field inside the (n+1)-st plasmoids is $\sim V_A$:

$$\delta B_y^{(n+1)} \sim \frac{\psi^{(n+1)}}{w^{(n+1)}} \sim V_A \Rightarrow w^{(n+1)} \sim \frac{\psi^{(n+1)}}{V_A} \qquad (233)$$

Finally,

$$\psi^{(n+1)} \sim \frac{\partial \psi^{(n+1)}}{\partial t} \cdot \frac{L^{(n)}}{V_A} \qquad (234)$$

travel time through the sheet (after which they are swallowed by the n-th plasmoid)

This gives

$$\frac{\partial \psi^{(n)}}{\partial t} \sim \frac{w^{(n+1)}}{L^{(n)}} V_A^2 \sim \frac{\psi^{(n+1)}}{L^{(n)}} V_A \sim \frac{\partial \psi^{(n+1)}}{\partial t} \qquad (235)$$

Thus, the reconnection rate is the same at every level! But this means that it is the same as the rate at the level of the critical sheet. (230).

So, the reconnection rate is only limited by the maximum reconnection rate in the largest possible stable SP sheet:

$$\left(\frac{\partial \psi}{\partial t}\right)_c \sim S_c^{-1/2} V_A^2 \sim 10^{-2} V_A^2 \quad (236)$$

- about ~100 times slower than ideal MHD dynamics, but independent of η!

This is fine observationally, although actually, it turns out that when non-MHD collisionless effects ~~are~~ are taken into account, it is possible to get reconnection rates that are ~10 times faster than this.

The above ~~theory~~ result is due to Uzdensky, Loureiro & AAS (2010), although the way in which I presented it here draws heavily on an earlier paper by Shibata & Tanuma (2001), which almost got there.

(236) was confirmed numerically by ~~B~~ Bhattacharjee et al (2009) & Loureiro et al (2012), and countless times since.

4.5.4 Plasmoid Distribution

There is a nice, testable (and tested, in the latter paper) ~~result~~ corollary. The # of plasmoids with $\psi > \psi^{(n+1)}$ is

$$N^{(n)} \sim \frac{L}{L^{(n)}} \underset{\substack{\uparrow \\ (234)}}{\sim} \frac{1}{\psi^{(n+1)}} \frac{\partial \psi^{(n+1)}}{\partial t} \frac{L}{V_A} \underset{\substack{\uparrow \\ (236)}}{\sim} \frac{L V_A}{\psi^{(n+1)}} S_c^{-1/2} \qquad (237)$$

So the fluxes in plasmoids have the distribution

$$f(\psi) = -\frac{dN^{(n)}}{d\psi} \propto \psi^{-2} \qquad (238)$$

In view of (233), the distribution of plasmoid widths is the same.

The reconnection process is scale-invariant and so is the plasmoid distribution — naturally.